



The author(s) shown below used Federal funding provided by the U.S. Department of Justice to prepare the following resource:

Document Title: Pre-grouping of Commingled Human Skeletal Remains by Elemental Analysis

Author(s): Matthieu Baudelet, Ph.D.

Document Number: 309970

Date Received: January 2025

Award Number: 15PNIJ-21-GG-04151-SLFO

This resource has not been published by the U.S. Department of Justice. This resource is being made publicly available through the Office of Justice Programs' National Criminal Justice Reference Service.

Opinions or points of view expressed are those of the author(s) and do not necessarily reflect the official position or policies of the U.S. Department of Justice.

Agency: NATIONAL INSTITUTE OF JUSTICE

Grant Number: 15PNIJ-21-GG-04151-SLFO

Project title: Pre-grouping of commingled human skeletal remains by elemental analysis

PI: Dr. Matthieu Baudelet

Submission date: November 25, 2024

DUNS Number:

EIN Number:

Recipient Organization: University of Central Florida, 4000 Central Florida Boulevard, Orlando
FL 32816

Recipient Account Number:

Grant period: 01/2022-06/30/2024

Reporting period end date: 06/30/2024

Signature of submitting official: AOR

Shannon M. Callahan,

Digitally signed by Shannon M.
Callahan, AOR
Date: 2024.11.25 10:47:18 -05'00'

Purpose and objectives of the project

The purpose of this study is to evaluate Laser-Induced Breakdown Spectroscopy (LIBS) as a useful tool for sorting commingled remains. LIBS technology provides an elemental profile of the material being analyzed, in this case, human bones. LIBS can determine the unique elemental profile of each individual, to help sort commingled remains.

The goal of this project was to develop a protocol to use the elemental profile obtain by a portable LIBS instrument to sort and reassociate commingled remains. This goal was fulfilled in 2 parts:

- Design of a classification to optimize sorting of commingled remains obtained at the FOREST facility
- Comparison of the elemental approach with traditional methods of sorting remains

Project Design

One challenge in forensic anthropological contexts is the reassociation of commingled skeletal remains in a fast, accurate, and non-destructive manner [1]. In some cases, it is difficult to identify a bone fragment from other materials, let alone reassociate bones from the same individual and perform osteological analyses [1-3]. Currently, common techniques used to reassociate commingled human skeletal remains include: 1) physical matching of bone fragments; 2) evaluating articular surfaces to examine joint congruence; 3) visual pair-matching of bilateral elements; 4) osteometric pair-matching; 5) evaluation of taphonomic patterns; and 6) DNA analysis [1, 3-5]. Unfortunately, most of these techniques are limited in their efficacy by one or more factors, such as context-specific taphonomic histories, length of analysis time, access to

specialized instrumentation, cost, destructive sample preparation, and the need for larger sections of bone or nearly complete remains [6]. Forensic scenarios involving cases of commingled human remains compound these difficulties, particularly in instances of mass casualty events resulting from both natural and human-made disasters [7, 8]. As a result of these limitations, as well as the complex contexts that result in commingled skeletal assemblages, forensic anthropologists would benefit from the development of additional tools to help with the reassociation of commingled skeletal remains.

Recently, numerous forensic investigators have begun using non-invasive elemental analysis techniques such as scanning electron microscopy with energy dispersive X-ray spectroscopy (SEM/EDS), X-ray fluorescence (XRF), laser ablation inductively coupled plasma mass spectrometry (LA-ICP-MS), and Fourier-transform infrared spectroscopy (FTIR) for a variety of investigative purposes related to providing information on the elemental composition of unknown samples [6, 9-12]. Presently, most elemental analyses of bones are conducted using portable XRF (pXRF), which can examine the elemental composition of a material in a non-destructive manner [9-12]. pXRF has been used to detect non-skeletal elements in cases of potentially contaminated cremated remains [10, 13], to separate osseous and dental tissues from other chemically similar materials [6], and to help resolve a case of small-scale commingling [3,17]. However, there are limitations to the elements XRF can detect without the need for additional equipment or analysis time, specifically elements with lower atomic masses.

Newly introduced to anthropological fields, including forensic anthropology, bioarchaeology, and zooarchaeology, laser-induced breakdown spectroscopy (LIBS) is similar to XRF in its ease of use, visually non-destructive analytical workflow, and the lack of sample preparation needed [15-18]. However, LIBS has the added ability to detect lower atomic weight

elements like carbon (C), nitrogen (N), and oxygen (O), which may be the key to differentiating individuals from one another [16]. Furthermore, LIBS can aid in the identification of human remains using laser ablation occurring at the micro-scale, making the technique visually non-destructive to the sample [15,16]. Recent contributions demonstrated the use of LIBS for associating human skeletal remains from multiple individuals. Siozos *et al.* [16] used LIBS to associate seven bone fragments from five human individuals, recovered from an archaeological context in the United Kingdom. The small size of their test set (2 bones) was not conclusive with one of them never assigned to the correct individual and the other being assigned with a 91% accuracy. Roldán *et al.* [17] tested LIBS on eight bones from four non-human individuals (one femur and one tibia for each) and showed an average validation training accuracy of 98%. Moncayo *et al.* [15] analyzed twenty-five bones from five human individuals (five bones each) recovered from a cemetery in Segovia, Spain. In this study, a neural network algorithm was used for the re-association of bones to their individual and the training validation showed an accuracy of 99%. They also expanded their work in the same study to twelve teeth from four other individuals (three incisors each), with a 99% training validation accuracy. Considering this previous body of work, LIBS has potential to offer a complementary method for reassociating human skeletal remains during the identification process.

Notably, these studies were performed with lab-based LIBS instruments. Such systems are designed for high resolution analysis and high control of the laser ablation, require wall-plug power and laboratory space of several square-meters to contain the instrumentation. These systems also often require the samples to be contained in a chamber, reducing the size of samples being analyzed to few centimeters, and prevent an easy control of the sample for analysis. Handheld LIBS

instruments are common alternatives that can be utilized in conditions where wall-plug power may not be easily available and are easily deployable in field recovery contexts [19].

This project has now brought the use of LIBS as a tool for the re-association of commingled remains to a new standard:

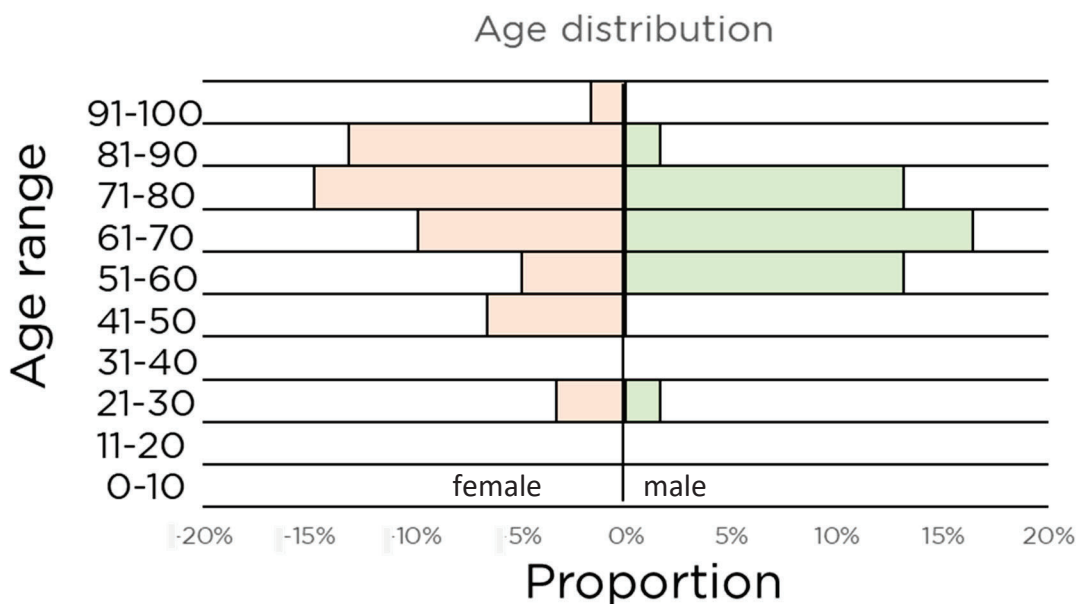
- It has been evaluated on 62 individuals
- It shows that LIBS can associate commingled remains in a supervised classification scheme with an accuracy of 87%

A. SAMPLE SET

The project utilized the John A. Williams Documented Human Skeletal Collection, casually known as the JAW Collection, currently housed in the Western Carolina Human Identification Lab (WCHIL) within the Department of Anthropology and Sociology at Western Carolina University (WCU). The JAW Collection was officially established in 2009 when the skeletal remains of the first donor at the Forensic Osteology Research Station (FOREST) arrived at the WCHIL for processing and curation. The collection was named for its founder John Allen Williams, a board-certified forensic anthropologist.

Sixty-two sets of skeletal remains were tested. In all phases, skeletons were chosen based on an equal ratio of males and females (biological sex based on death certificate, biological questionnaire completed by donor or his/her next of kin, and visual identification at intake), date of deposition, and recovery (occurring sometime during 2012 through 2022). Age at death continued to broaden with the addition of more individuals expanding the range to 28 to 100 years at death. Donor specific data of all donors sampled is provided in Annex 1. Donor #/Numbers are used to protect the privacy of the donor. Sex, date of birth, and date of death were all cross-checked with the death certificate and the biological questionnaire when possible. Placement and recovery dates were

recorded as part of the overall intake and recoveries processes; photographs were also taken on those and time stamps support that information. “Time at FOREST “ was calculated using the website timeanddate.com, date to date calculator¹ . FOREST Location indicates which of the two enclosures the individual was in. Enclosure 1 is where donor decompose on the surface. Enclosure 2 is where individuals are buried. All individuals for this study have come from Enclosure 1.



B. LIBS SPECTRA OF BONES

LIBS spectra were acquired using the SciAps Z300 portable LIBS unit in conjunction with the proprietary SciAps software Profile Builder. This instrument uses a 1064 nm Nd:YAG laser with an average pulse energy of 5 mJ and a spot size of 50-70 μm. It should be noted that the pulse energy and fluence of the laser within the SciAps Z300 cannot be manipulated by the user. The portable LIBS used in this study detects the UV-Vis-NIR spectral range of 188 to 950 nm, with a reported spectral resolution of 0.14 nm. This is achieved by three Czerny-Turner spectrometers

¹ <https://www.timeanddate.com/date/duration.html>

within the instrument. The instrument has a default gate delay setting of 650 ns and an integration period of 1 ms. Three linear CCD arrays coupled to the spectrometers are calibrated to detect the following wavelength ranges: (1) 188 to 365 nm, (2) 365 to 620 nm, and (3) 620 to 950 nm.

An averaged spectrum from 20 consecutive laser shots was acquired from the surface of each location using a 50 Hz pulse rate, after 5 cleaning shots were used to remove any surface contamination. Using a Keyence VHX-6000 Digital Microscope, the resultant ablation crater was measured to be approximately 180 μm in diameter with a depth of 125 μm . An example of a characteristic human bone spectrum, averaged from all spectra acquired in the study, is seen in Figure 1.

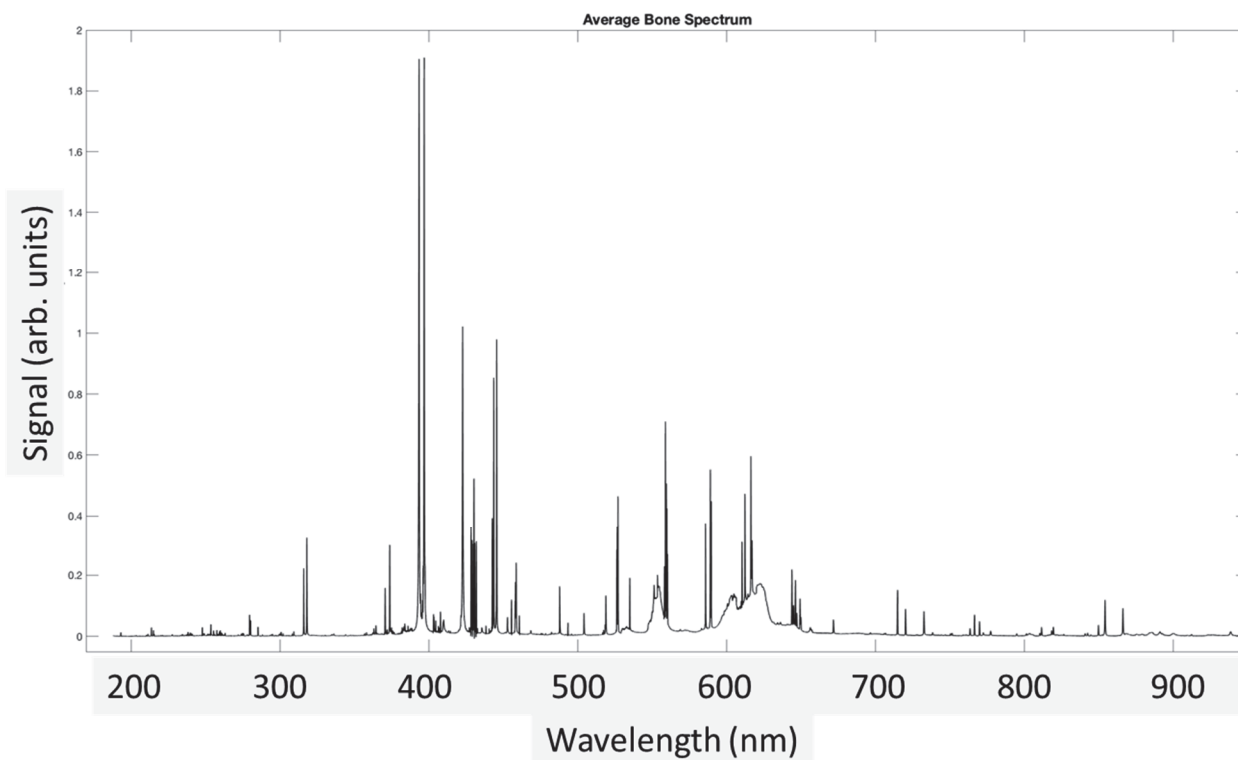


Figure 1. Average LIBS Spectrum of human bone

The major elements from the calcium hydroxyapatite (calcium, phosphorous, oxygen, hydrogen) and collagen (hydrogen, carbon, nitrogen, oxygen) matrix were detected. Major and minor elements [24] were also detected in the spectra: aluminum, barium, copper, iron, potassium, magnesium, sodium, silicon, strontium, zinc. Molecular bands of calcium hydroxide (CaOH) were also detected from the recombination of Ca, O, and H in the plasma (green and orange bands between 500 and 650 nm). Additional molecular signal from calcium fluoride (CaF) was detected between 529 and 535 nm, resulting from the recombination of calcium and fluorine atoms from the bone in the plasma. An inert argon gas flow was created within the instrument to remove interaction of the plasma with the atmosphere and stabilize its spectral emission. This resulted in argon emission lines, shown in Table 2, while not characteristic of the bone composition.

The major elements from the calcium hydroxyapatite (calcium, phosphorous, oxygen, hydrogen) and collagen (hydrogen, carbon, nitrogen, oxygen) matrix were detected. Major and minor elements [24] were also detected in the spectra: aluminum, barium, copper, iron, potassium, magnesium, sodium, silicon, strontium, zinc. Molecular bands of calcium hydroxide (CaOH) were also detected from the recombination of Ca, O, and H in the plasma (green and orange bands between 500 and 650 nm). Additional molecular signal from calcium fluoride (CaF) was detected between 529 and 535 nm, resulting from the recombination of calcium and fluorine atoms from the bone in the plasma. An inert argon gas flow was created within the instrument to remove interaction of the plasma with the atmosphere and stabilize its spectral emission. This resulted in argon emission lines, shown in Table 2, while not characteristic of the bone composition.

The list of elements and their spectral lines is listed below:

Element	Wavelength (nm)
---------	-----------------

Calcium	220.1, 227.6, 239.9, 299.5, 299.7, 300, 300.7, 300.9, 334.4, 335, 336.1, 347.5, 348.8, 362.4, 363.1, 364.4, 409.3, 409.5, 409.9, 410.9, 422.7, 428.3, 428.9, 429.9, 430.2, 430.7, 431.8, 435.6, 442.5, 443.5, 445.5, 452.7, 457.8, 458.1, 458.6, 468.5, 487.8, 504.2, 518.9, 526.2, 526.5, 527, 551.2, 558.2, 558.9, 559.4, 559.8, 560.1, 560.3, 585.7, 586.8, 610.2, 612.2, 616.2, 616.9, 631.7, 634.3, 636.1, 643.9, 644.9, 646.2, 647.1, 649.3, 649.9, 671.7, 714.8, 720.2, 732.6, 849.8, 854.2, 866.2, 210.3, 211.3, 219.8, 220.8, 315.9, 317.9, 318.1, 370.6, 373.7, 393.4, 396.8, 534.9
Phosphorous	202.3, 203.3, 213.6, 214.9, 215.4, 253.4, 253.5, 255.3
Oxygen	(777.2, 777.4, 777.5)*, 844.6
Hydrogen	486, 656,2
Carbon	193, 247.8, 833.4
Nitrogen	742.4, 744.3, 746.8
Aluminum	236.7, 237.3, 308.2, 309.3, 394.3, 396.1
Barium	553.5, 455.4, 493.4
Copper	324.7, 327.4
Iron	247.3, 248.3, 248.8, 249, 251.1, 252.3, 252.8, 271.9, 272.1, 302.1, 344.1, 357, 358.1, 361.9, 372, 374.9, 375.8, 381.6, 382, 382.6, 404.6, 438.3, 233.3, 234.3, 234.8, 236.5, 238.2, 238.9, 239.5, 240.5, 240.6, 241.1, 256.2, 258.6, 259.9, 260.7, 261.2, 261.4, 262.6, 262.8, 263.1, 273.9, 274.6, 274.9, 275.6
Potassium	766.49, 769.9
Magnesium	277.9, 278.3, 285.2, 382.9, 383.2, 383.8, 387.8, 516.7, 517.3, 518.4, 279.1, 279.5, 279.8, 280.2

This resource was prepared by the author(s) using Federal funds provided by the U.S. Department of Justice. Opinions or points of view expressed are those of the author(s) and do not necessarily reflect the official position or policies of the U.S. Department of Justice.

This resource was prepared by the author(s) using Federal funds provided by the U.S. Department of Justice. Opinions or points of view expressed are those of the author(s) and do not necessarily reflect the official position or policies of the U.S. Department of Justice.

Sodium	568.2, 568.8, 589, 589.6, 818.3, 819.5
Silicon	243.5, 250.7, 251.4, 251.6, 251.9, 252.9, 288.1
Strontium	407.7
Zinc	213.9, 468, 472.2, 481.1, 206.2
Argon (purging gas)	675.3, 687.1, 693.8, 696.5, 706.7, 714.8, 727.3, 737.2, 750.4, 751.4, 763.5, 772.4, 794.8, 800.6, 801.4, 810.3, 811.5, 826.4, 840.8, 842.4, 852.1, 866.1, 866.8, 912.2, 922.4
CaOH	Around 554 nm, 623 nm
CaF	Bandheads at 529 nm, 606.4 nm.

The crucial aspect of not altering the bone during the LIBS analysis was evaluated. The result of the laser ablation (5 cleaning laser shots followed by 10 laser shots to create the analytical plasmas) is shown in Figure 3. The bone used for this measurement was a deer rib, as we could not transfer the human remains to the digital microscope (VHX-6000, Keyence) and a laser confocal microscope (VK-X3000, Keyence) used for the visual analysis.

The laser-induced crater is 90 μm deep and $120 \times 150 \mu\text{m}^2$ large on the surface of the bone. This corresponds to a removal of approximately 6 micrometers of material per laser shot in depth. The laser-induced ablation is not visible to the naked eye. Resultantly, LIBS analysis can be considered a visually non-disruptive method of taking chemical measures of bone.

LIBS relies on the sampling and excitation of the ablated material by a laser pulse. As shown in Figure 4, while there is sample removal, the sampling is not visible to the naked eye and can be considered visually non-disruptive.

LIBS spectral data were acquired after laser ablation removed 30 μm of cortical bone surface from each sampling location. This “cleaning” step is used to remove surface contamination from the depositional environment. Postmortem diagenetic changes to cortical bone surfaces are known to penetrate bone surfaces from hundreds of micrometers to a few millimeters [16]. In this pilot study, diagenetic changes were minimized by testing the LIBS instrument on contemporary bone samples derived from surface placements at an outdoor decomposition facility. Future studies testing LIBS should be conducted on skeletal elements recovered from burial environments to determine how much diagenetic changes to bone remain can be a concern for LIBS studies, especially when postmortem environments penetrate more than a few μm of the cortical bone surface.

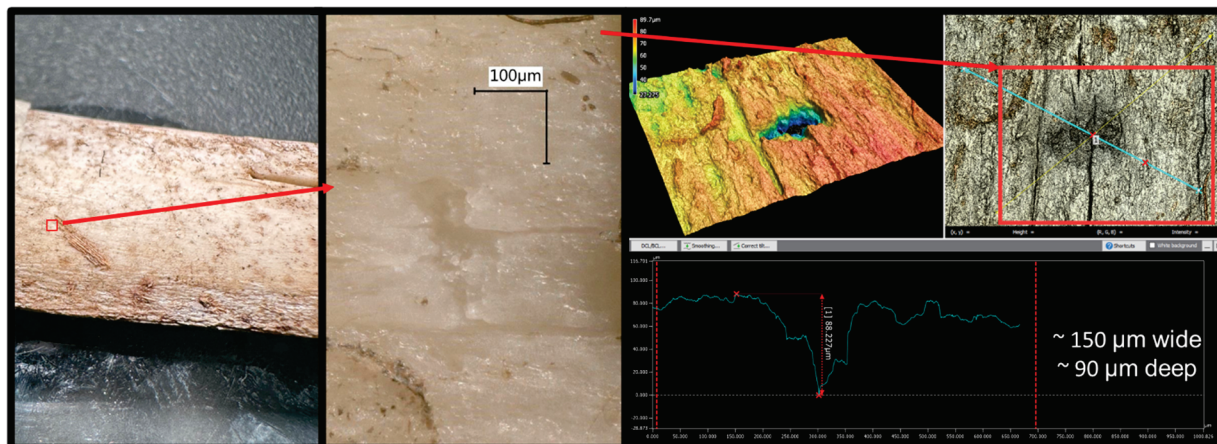


Figure 2. Microscopical analysis of the laser-induced ablation left after LIBS analysis of a bone

Thirty-five (35) bones per individual were selected for analysis to maximize skeletal representation, including both large and small bones from the midline and appendicular skeleton (Figure 3). Between 1 and 13 locations were sampled on each bone, depending on their size, mimicking the sampling of bone fragments (see Annex 2 for the full list of sampling locations). While the target number of bones to be sampled from each individual was 35, the incompleteness

This resource was prepared by the author(s) using Federal funds provided by the U.S. Department of Justice. Opinions or points of view expressed are those of the author(s) and do not necessarily reflect the official position or policies of the U.S. Department of Justice.

This resource was prepared by the author(s) using Federal funds provided by the U.S. Department of Justice. Opinions or points of view expressed are those of the author(s) and do not necessarily reflect the official position or policies of the U.S. Department of Justice.

of the skeletal remains (e.g., the common absence of hand and foot bones) made the actual number of bones examined per individual range from 4 to 35, with a median value of 29 bones per individual (See Annex 3 for inventory of bones sampled for each individual).

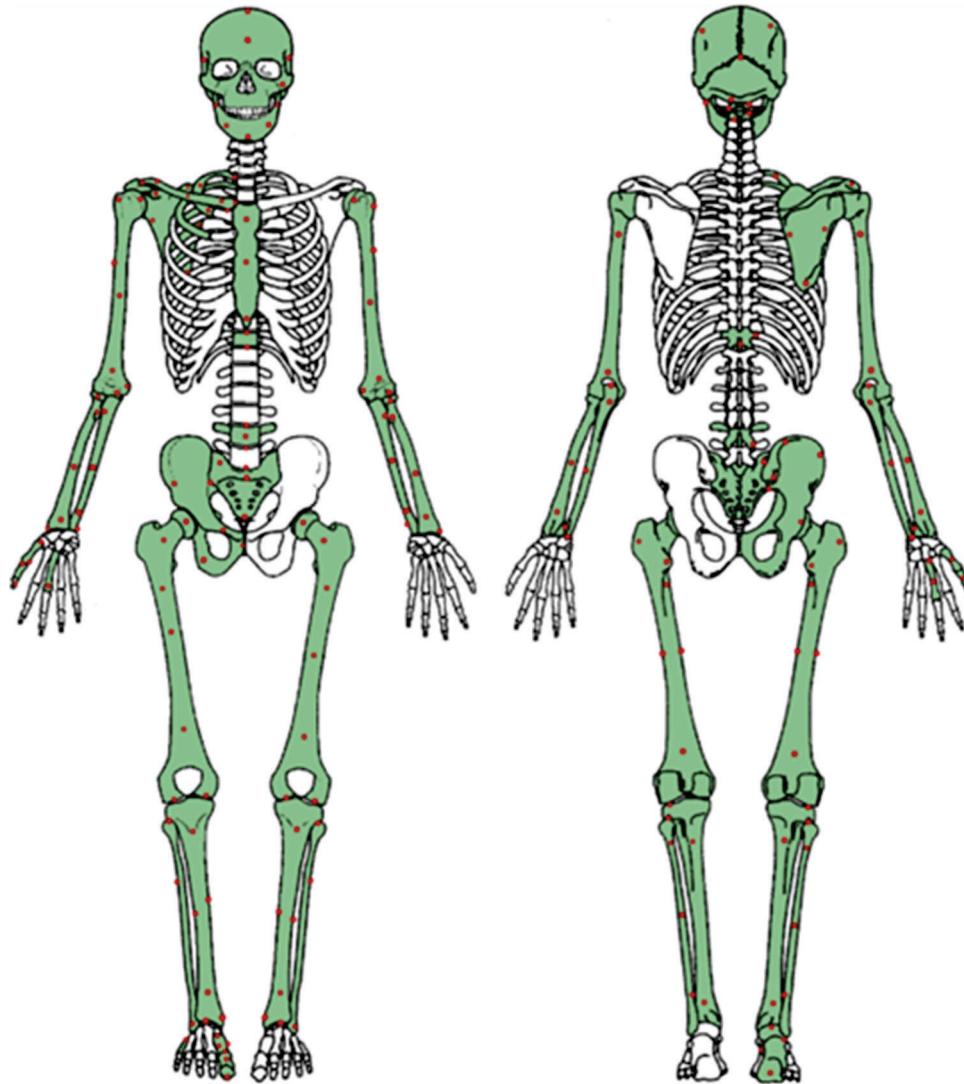


Figure 3. Skeletal locations for LIBS sampling. Shaded bones selected for analysis. Filled circles indicate the sites of spectral acquisition

C. REASSOCIATION OF INDIVIDUALS BY PCA-LDA

This resource was prepared by the author(s) using Federal funds provided by the U.S. Department of Justice. Opinions or points of view expressed are those of the author(s) and do not necessarily reflect the official position or policies of the U.S. Department of Justice.

This resource was prepared by the author(s) using Federal funds provided by the U.S. Department of Justice. Opinions or points of view expressed are those of the author(s) and do not necessarily reflect the official position or policies of the U.S. Department of Justice.

Linear discriminant analysis (LDA) was used to construct a classification model for the 45 individuals based on the full LIBS spectrum. This model (as well as all others described in this study) was built using a stratified training and test set, split at a 70:30 ratio. A 30% holdout cross-validation was performed on the training models to evaluate classification loss and assess the potential for overfitting in the test data.

Data reduction was performed via Principal Component Analysis (PCA). LDA models were trained, cross-validated, and tested using an increasing number of principal components (PCs) as input variables. This process led to determining the number of PCs necessary for optimal classification accuracy for the dataset.

Due to the lack of chemical information represented in the simplified PCA score matrix, PCA was alternatively used as a feature selection tool to determine which spectral variables held the most valuable information for classification. The magnitude of eigenvalues within the PCA loadings was used to identify the specific wavelengths exhibiting the greatest variation among spectral profiles. The wavelengths were ranked based on their contribution to spectral variation and only the wavelength predictors with a contribution of 50% or higher were selected for further LDA trials. As a result, the final LDA models in this study were constructed with the reduced spectral data themselves, rather than transformed PCA score vectors.

Overall, the data collection, processing, and analysis is very efficient. Without the need for sample preparation, the ablation and acquisition process last approximately 10 seconds per accumulated spectrum. Each bone can be fully sampled between 1 and 3 minutes, depending on the number of spectra acquired per bone. Importing, pre-processing of data, and the PCA analysis requires around 30 minutes maximum. Non-reduced LDA model training and testing requires around 20 minutes. However, LDA using reduced datasets such as PCA score vectors or PCA-selected predictors can

be completed less than 20 seconds. In comparison with other physical reassociation methods that may take weeks, months, or even years to perform on such a large scale, the LIBS sorting process can be performed in a timelier manner.

The PCA loadings reveal specific wavelengths that present the most variation across all the bones' spectral profiles. By only retaining the wavelengths determined by PCA to have the highest variation and removing, or "masking," the noisy and redundant variables, the spectral data is significantly reduced. The original 22788 wavelength predictors were reduced to 297 wavelength predictors – 1.3% of the original input. These 297 variables correspond to 28 distinct emission lines (Table 1). Figure 4 highlights the data reduction that occurs through this process, with only the colored emission lines used for subsequent data analysis. Using the spectral information from these selected inputs alone, the bone profiles were assigned to their respective individuals via LDA with an overall accuracy of 87%. This method not only matches the success rate of the traditional PCA-LDA algorithm shown above, but it takes it a step further by delineating the spectral regions centered on specific emission lines that discriminates among individuals' remains. By defining

which variables are important for individual classification, the mask could be applied to entirely new sets of human skeletal data, greatly simplifying the process of spatial reduction for future datasets.

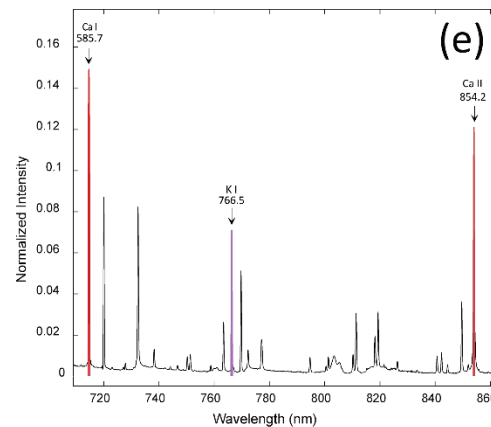
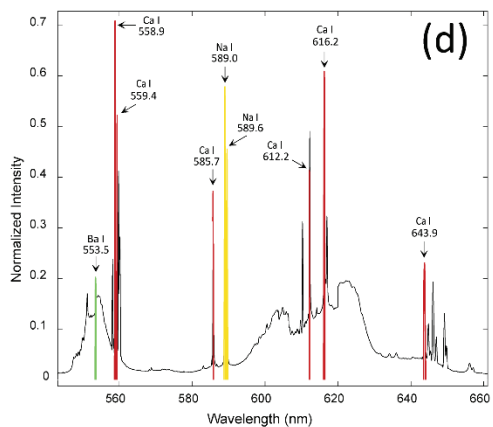
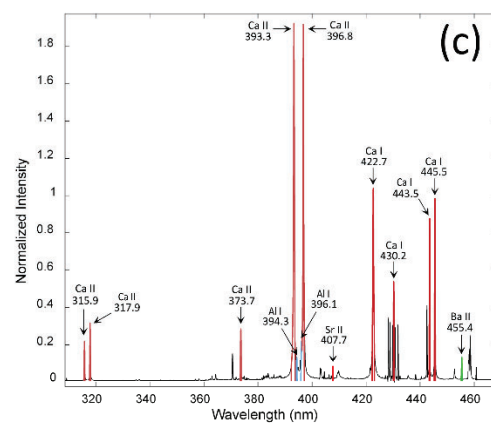
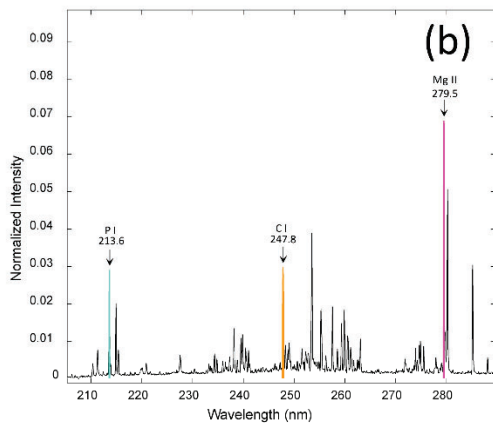
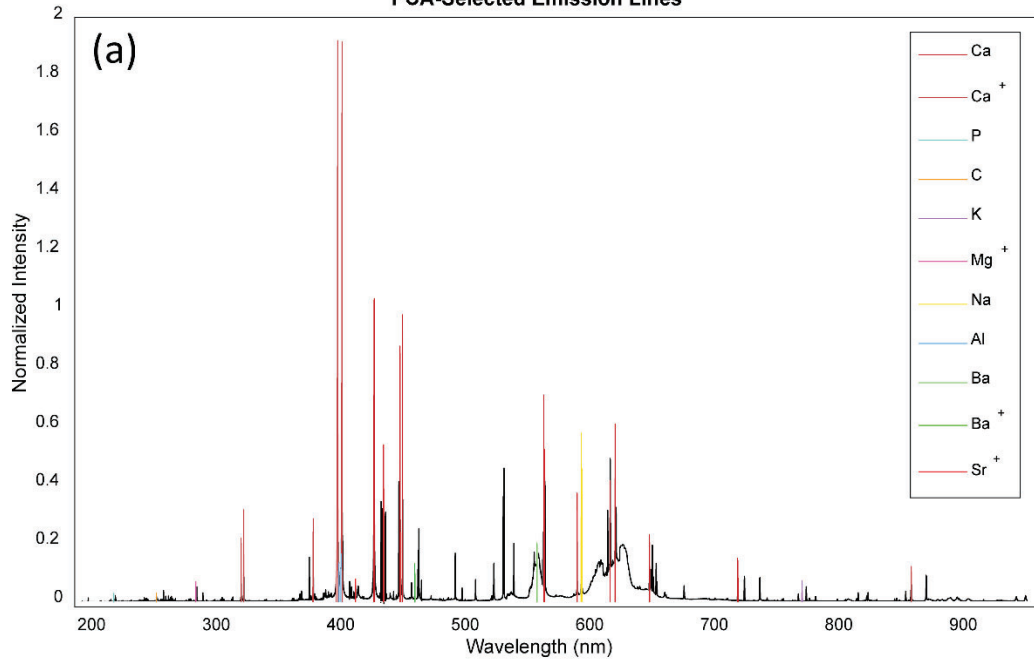
Table 1. List of PCA-selected LIBS Emission Lines

Element	LIBS Emission Wavelength (nm) *indicates singly ionized element
Aluminum	394.3, 396.1
Barium	455.4*, 553.5
Calcium	315.9*, 317.9*, 373.3*, 393.3*, 396.8*, 422.7, 430.2, 443.5, 445.5, 558.9, 559.4, 585.7, 612.2, 616.2, 643.9, 714.8, 854.2*
Carbon	247.8
Magnesium	279.5*
Phosphorus	213.6
Potassium	766.5
Sodium	589.0, 589.6
Strontium	407.7*

This resource was prepared by the author(s) using Federal funds provided by the U.S. Department of Justice. Opinions or points of view expressed are those of the author(s) and do not necessarily reflect the official position or policies of the U.S. Department of Justice.

This resource was prepared by the author(s) using Federal funds provided by the U.S. Department of Justice. Opinions or points of view expressed are those of the author(s) and do not necessarily reflect the official position or policies of the U.S. Department of Justice.

PCA-Selected Emission Lines



This resource was prepared by the author(s) using Federal funds provided by the U.S. Department of Justice. Opinions or points of view expressed are those of the author(s) and do not necessarily reflect the official position or policies of the U.S. Department of Justice.

This resource was prepared by the author(s) using Federal funds provided by the U.S. Department of Justice. Opinions or points of view expressed are those of the author(s) and do not necessarily reflect the official position or policies of the U.S. Department of Justice.

Figure 4. PCA-selected spectral emission lines used for LDA modeling. 4a presents the selected spectral features overlaid onto the full average LIBS spectrum of human bone. 4b - 4e highlight the 28 selected emission lines

The classification results of the LDA model using the PCA-selected predictors are visualized using graph theory in Figure 5, which is based upon the test set confusion matrix. Each individual is represented as a numbered node. The color of each node represents the classification accuracy associated with the bones of that individual's remains. If a spectrum has been misclassified as belonging to another individual, this is represented as a directional edge, where an arrow points towards the individual to which the spectrum was incorrectly assigned. The thickness of an edge is proportional to the number of misclassifications occurring between two individuals.

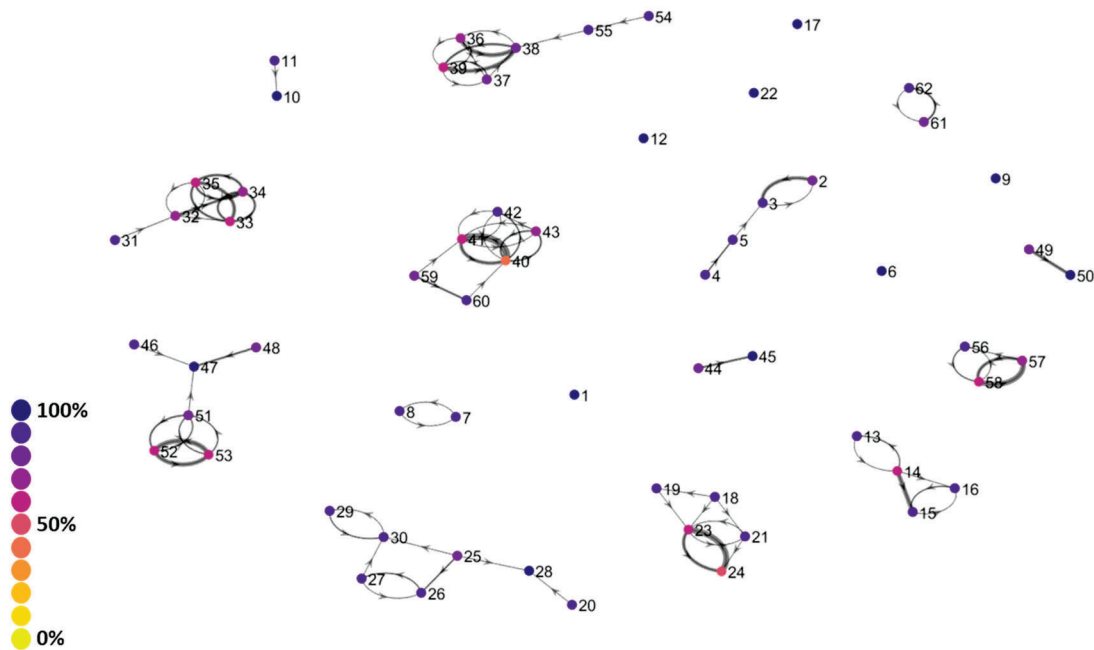


Figure 5. LDA classification plot for 62 sets of skeletal remains. Each dot represents an individual. Color indicates classification accuracy. Directed arrows indicate a misclassification; arrow weight represents degree of misclassification.

D. COMPARISON WITH TRADITIONAL ANTHROPOLOGICAL METHOD

The purpose of the research is to investigate the accuracy of human-attempted sorting of human skeletal remains compared to sorting via laser-induced breakdown spectrometry (LIBS). The goal is to find the strengths and weakness in each approach so that a new method that combines both approaches can be developed.

The study took place at Western Carolina University in the Western Caroline Human Identification Lab (WCHIL). Five skeletons from the John A. Williams Documented Human Skeletal Collection (JAW collection) were selected. They had previously been sampled with the LIBS machine and are part of that database. Bones that were not selected for the human-bone reassociation study were resampled as part of this phase of the project. All donors were adults, three females and two males. Specific bones, meant to represent a range of skeletal elements, were chosen from each individual. The goal was to provide the anthropologist with a range of bones to work with thus allowing us to see if there was a pattern to which bones were more correctly associated over other. Remains were also chosen to represent a variety of clues for the anthropologist to find such as ability to articulate bones, robusticity, and taphonomic modifications. Challenging bones, like metacarpals or an isolated long bone were selected to challenge the anthropologist and with zero expectation that they would get those correct. 100 bones were chosen from across the five donors. Table 2 lists which skeletal remains will be selected from each donor.

Table 2. Skeletal remains chosen from each donor

Donor 1	Donor 2	Donor 3	Donor 4	Donor 5
humerus	scapula	rib3-8	femur	tibia
innominate	rib3-8	rib 1	fibula	T12
rib 1	fibula	rib3-8	MT 2	rib 1
radius	rib3-8	T1	femur	talus
clavicle	L1-4	clavicle	MT1	manubrium
radius	L5	T1	innominate	humerus
rib 1	innominate	cranium	clavicle	scapula

talus	calcaneus	C3-6	patella	cuboid
MT	tibia	T	cranium	mandible
hand phalanx	talus	C1	MT5	t
hand phalanx	rib3-8	c3-6	scaphoid	sacrum
femur	sacrum	rib 2 or 3	mandible	scaphoid
c1	ulna	C3-6	tibia	t-fused
mandible	foot phalanx	rib 2 or 3	humerus	rib 2
mc1	mc1	C7	ulna	mt4
c2	mc4	rib 2		mt5
scapula	mc5	C2		mt3
clavicle	mc2	scapula		
sacrum	mandible	rib3-8		
cervical fused	L5	rib1		
	humerus	c3-6		
	clavicle	scapula		
	patella	ulna		
	fibula	femur		

Once the 100 bones had been chosen, they were put on a large table and commingled. Electrical tape was then applied to cover the donor-specific catalog number written on each bone. The bones were then numbered 1-100. A spreadsheet was maintained that documented the donor-specific catalog number, the bone, side, and number that was written on the electrical tape.

Participants were told to sort the commingled remains into individuals. The instructions were intentionally left vague to simulate working with a range of skeletal experts and their varying backgrounds and training. There was also no scenario attached to the skeletal remains to suggest reason for commingling, context of recovery, or any possible demographic information. The anthropologists did not know that the remains came from five individuals, we wanted them working with an open population.

Five anthropologists participated in the study. All had between 7 and 20 years of experience working with skeletal remains in forensic and archaeological contexts. They ranged in specialization from primarily forensic anthropology training and practice to primarily bioarcheological training and practice. Both specialties receive similar training in skeletal analysis, but their goals are different. Forensic anthropologists have the added pressure of working with contemporary people and the outcomes of incorrect reassociation. Bioarcheologists impact contemporary people with their handling and analysis of skeletal remains but the consequences of incorrect reassociation are not as severe.

Each anthropologist approached the study differently, which is a useful but limiting. For example, the first participant only associated remains that they felt very confident about and left the rest untouched. They made 17 groups of bones, associating 53 of the 100 bones. 51 of the 53 bones were correctly matched to one or more bones from the same individual resulting in a 96% success rate. 47 bones were not touched. It should be noted that this participant reported about 20 years of experience. Alternatively, two participants, made five groups and put all 100 bones into one of those five groups. These two participants were about successful with ~60% of the remains. In each case, there were subgroups within each primary group that were correct. For example, if the participant grouped 20 bones in a pile. Ten of them go with each other. Seven of them go with

each other but not with the groups of ten. Three of the 20 do not go with either the ten or seven sub-group. When the subgroups were considered separate groups, rather than one individual, correct association goes up to ~75%. The final two participants were less confident and did a combination of the two approaches discussed above. They made several separate groups and left some remains unassociated. This approach was successful at about 68%. The general conclusion to be drawn from this is that the anthropologist should only make associations that they feel confident about. This study asked about confidence of association in quartiles, but future work should set the standard higher at 85% or 90% confidence. In each case, the smaller groupings were more accurate. Post-sort interviews with each participant also demonstrated that they each had reassociations they felt good about and others that they felt less confident about but still grouped them as being the same individual.

Post-sorting interviews indicated that anthropologists primarily used an assessment of articulation between bones and taphonomic modification as their primary clues for reassociation. They all noted that taphonomic modification is an unreliable indicator but a few of the remains had an unusual blue staining on them and a few others had the same animal-induced fracture pattern. At the beginning of the study, it was hypothesized that the anthropologists would more frequently, correctly reassociate long bones and vertebrae that could be more easily articulated. Analysis of bone type and frequency of correct association showed that isolated bones like patellae, metacarpals, and metatarsals were not correctly associated, or chosen for association, by any of the anthropologists. Conversely, many of the ribs and vertebrae were correctly associated with at least one other bone from the same person 100% of the time. The long bones of the arms and legs were most frequently associated with at least one other bone from the same person 40-60% of the time.

For the LIBS analysis, being a supervised approach, 10 bones per individual, from the remaining skeletal sets, were chosen at random to be used as the training data. The training spectra for each individual was taken in the following randomized order on a single day.

Individual 4

1. L Ulna
2. Sacrum
3. L Os Coxa
4. R Fibula
5. Lumbar 4
6. R Rib 3
7. L Tibia
8. Cervical 3
9. R Triquetrum
10. R Calcaneus

Individual 5

1. Thoracic 4
2. Sternum
3. L Os Coxa
4. Lumbar 1
5. L Radius
6. R Clavicle
7. Left 3rd Cuneiform
8. R Metatarsal 1

9. R Fibula

10. L Tibia

Individual 3

1. R Radius

2. L Ulna

3. L Fibula

4. Thoracic 5

5. R Femur

6. R Clavicle

7. R Cuboid

8. R Tibia

9. R Rib (between 7 to 9)

10. L Humerus

Individual 1

1. L Scapula

2. Cranium

3. Thoracic 5

4. Sternum

5. Cervical (between 3 to 6)

6. R Ulna

7. R Metacarpal 3

8. L Os Coxa

9. L Femur

This resource was prepared by the author(s) using Federal funds provided by the U.S. Department of Justice. Opinions or points of view expressed are those of the author(s) and do not necessarily reflect the official position or policies of the U.S. Department of Justice.

This resource was prepared by the author(s) using Federal funds provided by the U.S. Department of Justice. Opinions or points of view expressed are those of the author(s) and do not necessarily reflect the official position or policies of the U.S. Department of Justice.

10. R Humerus

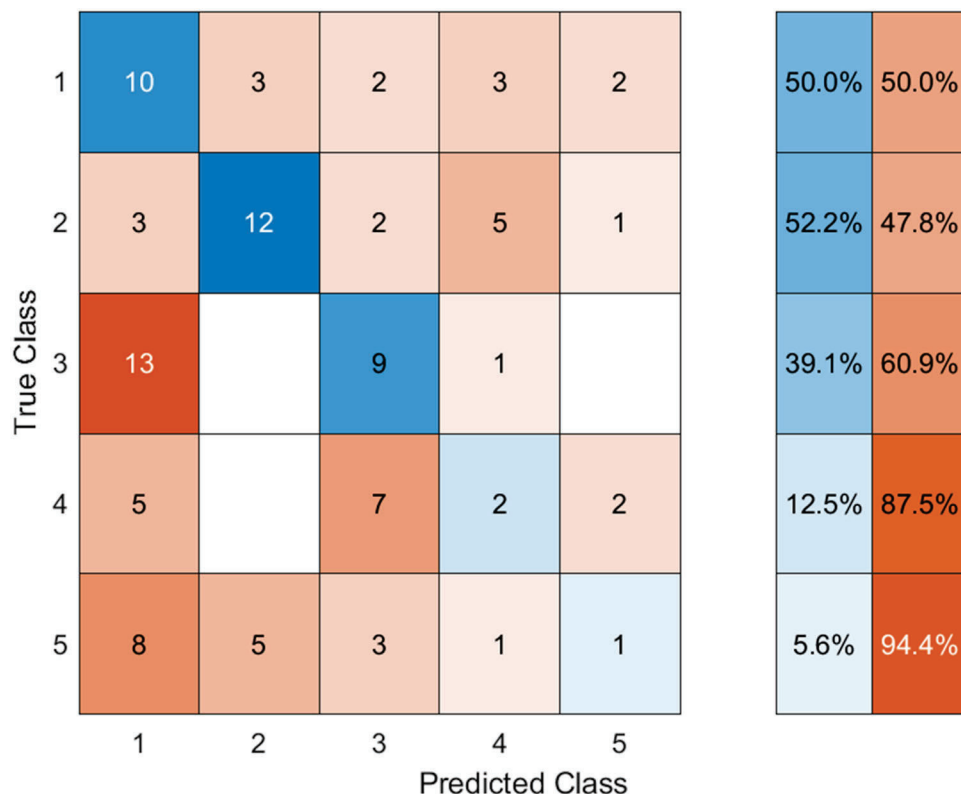
Individual 2

1. L Metacarpal 1
2. R Scapula
3. L Capitate
4. L Tibia
5. L Fibula
6. R Metatarsal 2
7. L Radius
8. R Os Coxa
9. Cervical 1
10. L Ulna

The test set is comprised of the 100 pre-selected bones listed previously. LIBS data was collected from the 100 test bones on a single day (but not the same day as training data). The identity of each bone was unknown at the time of data acquisition. Based on findings from the study on 60 individuals, instrument wavelength calibration was performed by the user after data acquisition. This ensures there are no time-specific shifts present in the spectral data.

The final, processed spectral data used for data analysis contains 5893 input variables ranging from 187.31 nm to 951.77 nm (significantly reduced from the previous 12,000+ wavelength inputs). Data was normalized to the 534.9 nm Ca I line (a non-resonant emission line that consistently represents the bone matrix)

The reassociation results show that for the LDA (pseudolinear DA used due to the normalization) on 5893 variables (full spectra), a 34% accuracy overall was obtained, with the highest individual accuracy being 52%, lowest 5%



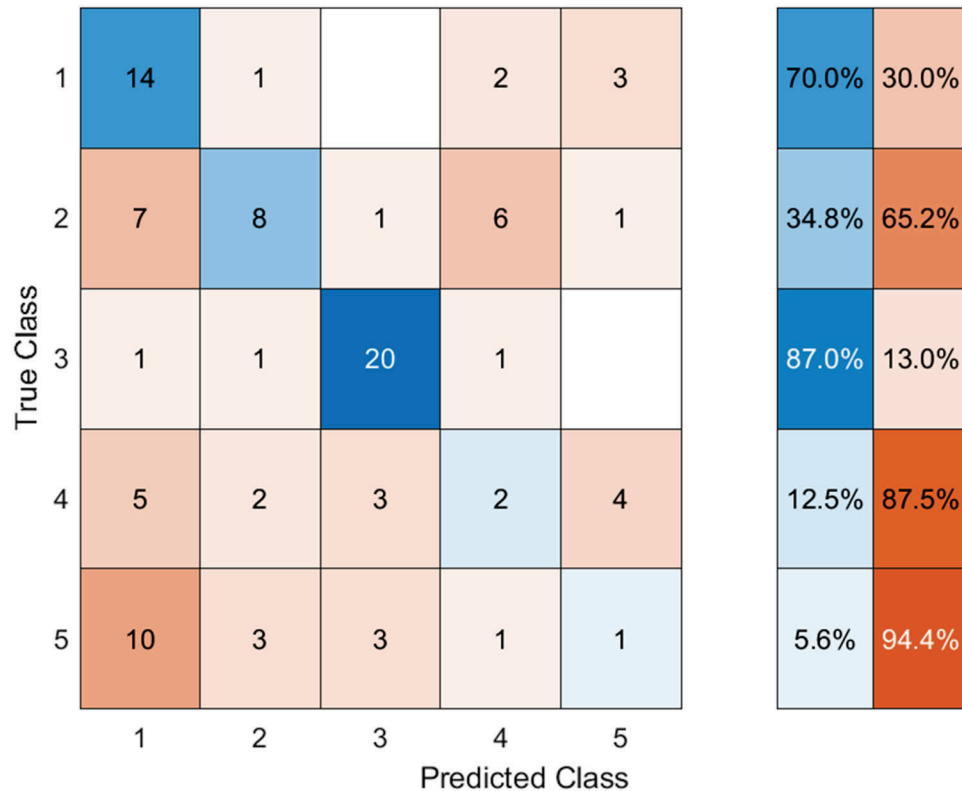
Using the spectral mask explained previously, 22 emission lines were found to be important for classification.

Element	Emission line
	*indicates singly ionized
Calcium	317.9*, 393.5*, 396.9*, 422.9, 443.7, 445.6, 558.8, 585.8, 612.4, 616.5, 644.1, 646.3, 715.0, 732.7, 854.2
Potassium	766.6, 769.9
Sodium	589.0, 589.7
Strontium	460.87

This resource was prepared by the author(s) using Federal funds provided by the U.S. Department of Justice. Opinions or points of view expressed are those of the author(s) and do not necessarily reflect the official position or policies of the U.S. Department of Justice.

This resource was prepared by the author(s) using Federal funds provided by the U.S. Department of Justice. Opinions or points of view expressed are those of the author(s) and do not necessarily reflect the official position or policies of the U.S. Department of Justice.

Barium	455.5*, 553.5
--------	---------------



Individuals 1 and 3 increased in accuracy, but individual 2 decreases in accuracy. No change were observed in individuals 4 and 5

The anthropologists performed with a success rate of 50% to 96%. The higher success was when the anthropologist made small groupings of remains that they felt 75% or more confident about. Furthermore, it was found that the bones most frequently reassociated correctly were the vertebrae and ribs and not the long bones. It is recommended that if the LIBS approach is learning from the anthropologist to build a profile for an individual, the technician should preference reassociations the anthropologist has high confidence about and within those, reassociations with vertebrae and ribs.

Implications for Criminal Justice Policy and Practice in the U.S.

The project confirms the successful application of handheld laser-induced breakdown spectroscopy (LIBS) to classify human remains based on their elemental signature with an accuracy higher than 90% using Linear Discriminant Analysis. While LIBS has previously shown its potential for such application, this project started a larger effort that shows that (1) it can be applied in the field thanks to its portability, and that (2) it does not require classification algorithms such as artificial neural networks that can be computationally intensive, preventing portability. The analysis is also shown to be minimally invasive for the bone. This allows for any further analysis by anthropologists and archaeologists to not be disturbed.

Scholarly products

PEER-REVIEWED PUBLICATIONS

1. Kristen Livingston, Katie Zejdlik, Matthieu Baudalet, “Reassociation of skeletal remains using laser-induced breakdown spectroscopy”, *Analytical Chemistry* 2024 96 (23), 9478-9485

PROCEEDINGS

1. Xenia Paula Kyriakou, Nicholas V. Passalacqua, Matthieu Baudalet, “The Right to the Truth: A Multimodal Investigation of Mass Graves and an Analysis of Commingled Remains for Conflict Resolution in Humanitarian Forensics”, *American Academy of Forensic Sciences - Anthropology*, paper A87

This resource was prepared by the author(s) using Federal funds provided by the U.S. Department of Justice. Opinions or points of view expressed are those of the author(s) and do not necessarily reflect the official position or policies of the U.S. Department of Justice.

This resource was prepared by the author(s) using Federal funds provided by the U.S. Department of Justice. Opinions or points of view expressed are those of the author(s) and do not necessarily reflect the official position or policies of the U.S. Department of Justice.

2. Kristen Livingston, Katie Zejdlik, Jonathan Bethard, Matthieu Baudelet, “The Chemical Reassociation of Commingled Remains Via Laser-Induced Breakdown Spectroscopy”, American Academy of Forensic Sciences - Anthropology, paper A93
3. Kristen Livingston, Matthieu Baudelet, Jonathan Bethard, Katie Zejdlik-Passalacqua, “The Rapid Association of Commingled Remains”, American Academy of Forensic Sciences - Anthropology, paper A49

PRESS RELEASES

1. Brian Didlake, “UCF professor looks to identify unknown remains using laser technology”, WKMG-TV, 12/07/2022 UCF professor looks to identify unknown remains using laser technology - YouTube
2. Jane Kim, “UCF professor’s research hopes to give closure for unidentified victims”, Orlando Sentinel, 12/07/2022 UCF professor’s research can sort bones in mass graves (orlandosentinel.com), video: <https://www.youtube.com/watch?v=AsHxQEhkz7w>
3. Jordan McGrew, “UCF Research Seeks to Give Families Closure by Developing Tools to Help Identify Individuals in Mass Graves”, UCF Today, 04/18/2022 UCF Research Seeks to Give Families Closure by Developing Tools to Help Identify Individuals in Mass Graves | University of Central Florida News
4. Case Hannum, “UCF chemistry professor receives grant to research method of sorting commingled remains”, NSM Today, 02/20/2022 UCF chemistry professor receives grant to research method of sorting commingled remains | News | NSM.today

PRESENTATIONS

This resource was prepared by the author(s) using Federal funds provided by the U.S. Department of Justice. Opinions or points of view expressed are those of the author(s) and do not necessarily reflect the official position or policies of the U.S. Department of Justice.

This resource was prepared by the author(s) using Federal funds provided by the U.S. Department of Justice. Opinions or points of view expressed are those of the author(s) and do not necessarily reflect the official position or policies of the U.S. Department of Justice.

1. Kristen Livingston, Matthieu Baudelet “Statistical Sorting of Commingled Remains Using Portable LIBS”, SciX 2022; 10/03/2022; Covington, KY, USA.
2. Kristen Livingston, Katie Zejdlik, Jonathan Bethard, Matthieu Baudelet, “The Chemical Reassociation of Commingled Remains Via Laser-Induced Breakdown Spectroscopy”, AAFS 2024; 02/22/2024; Denver, CO, USA
3. Matthieu Baudelet, “Pre-Grouping of Commingled Remains Using Field-Deployable Elemental Analysis”, AAFS 2024, National Institute of Justice Forensic Science Research and Development Symposium; 02/20/2024; Denver, CO, USA.
4. Kristen Livingston, Grace Myers, Katie Zejdlik, Jonathan Bethard, Matthieu Baudelet, “The Rapid Association of Commingled Remains”, AAFS 2023; 02/16/2023; Orlando, FL, USA.
5. Kristen M. Livingston, Matthieu Baudelet, Nicholas V. Passalacqua, Katie Zejdlik and Jonathan Bethard, “Resolution of commingled human remains using their elemental profile by Laser-Induced Breakdown Spectroscopy, 93rd Annual Meeting of the American Association of Biological Anthropologists; 03/20-23/2024; Los Angeles, CA, USA (poster)
6. Katie Zejdlik, Kristen Livingston, Grace Meyers, Jonathan D. Bethard, and Matthieu Baudelet. “Use of Laser-Induced Breakdown Spectrometry (LIBS) in Sorting Commingled Human Remains.” 92nd Annual Meeting of the American Association of Biological Anthropology; 04/19-22/2023 Reno, NV, USA
7. Kristen Livingston, “Rapid Association of Commingled Remains by their Chemical Profile”, ”, AAFS 2023, National Institute of Justice Forensic Science Research and Development Symposium; 02/14/2023; Orlando, FL, USA. (poster)

This resource was prepared by the author(s) using Federal funds provided by the U.S. Department of Justice. Opinions or points of view expressed are those of the author(s) and do not necessarily reflect the official position or policies of the U.S. Department of Justice.

This resource was prepared by the author(s) using Federal funds provided by the U.S. Department of Justice. Opinions or points of view expressed are those of the author(s) and do not necessarily reflect the official position or policies of the U.S. Department of Justice.

8. Matthieu Baudelet, Kristen Livingston, Katie Zejdlik, Jonathan Bethard, Nicholas Passalacqua, “Sorting commingled remains using their chemical profile”; DPAA - Joint Base Pearl Harbor-Hickam; 04/09/2024; Pearl Harbor, HI, USA (seminar)
9. Kristen Livingston, Matthieu Baudelet, “Advances in Chemical Sorting of Commingled Remains”, National Institute of Justice R&D Webinar Series, Forensic Technology Center of Excellence; 11/30/2023 (seminar)

REFERENCES

1. Adams, B., & Byrd, J. (Eds.). (2014). *Commingled Human Remains: Methods in Recovery, Analysis, and Identification*. Oxford, UK: Academic Press.
2. Bourgeois, R. L., Bazaliiskii, V. I., McKenzie, H., Clark, T. N., & Lieverse, A. R. (2021). A four-stage approach to re-associating fragmented and commingled human remains. *Journal of Archaeological Science: Reports*, 37, 102984.
3. Finlayson, J. E., Bartelink, E. J., Perrone, A., & Dalton, K. (2017). Multimethod resolution of a small-scale case of commingling. *Journal of Forensic Sciences*, 62(2), 493-497.
4. Adams, B., & Konigsberg, L. (2008). How many people? Determining the number of individuals represented by commingled human remains. In *Recovery, analysis, and identification of commingled human remains* (pp. 241-255): Springer.
5. Herrmann, N. P., & Devlin, J. B. (2008). Assessment of commingled human remains using a GIS-based approach. In *Recovery, analysis, and identification of commingled human remains* (pp. 257-269): Springer.
6. Zimmerman, H. A., Meizel-Lambert, C. J., Schultz, J. J., & Sigman, M. E. (2015). Chemical differentiation of osseous, dental, and non-skeletal materials in forensic anthropology using elemental analysis. *Science & Justice*, 55(2), 131-138.
7. de Boer, H. H., Roberts, J., Delabarde, T., Mundorff, A. Z., & Blau, S. (2020). Disaster victim identification operations with fragmented, burnt, or commingled remains: experience-based recommendations. *Forensic Sciences Research*, 5(3), 191-201.
8. Kontanis, E. J., & Sledzik, P. S. (2014). Resolving commingling issues during the medicolegal investigation of mass fatality incidents. In B. J. Adams & J. E. Byrd (Eds.), *Commingled Human Remains: Methods in Recovery, Analysis, and Identification* (pp. 447-468): Elsevier.

This resource was prepared by the author(s) using Federal funds provided by the U.S. Department of Justice. Opinions or points of view expressed are those of the author(s) and do not necessarily reflect the official position or policies of the U.S. Department of Justice.

This resource was prepared by the author(s) using Federal funds provided by the U.S. Department of Justice. Opinions or points of view expressed are those of the author(s) and do not necessarily reflect the official position or policies of the U.S. Department of Justice.

9. Christensen, A. M., Smith, M. A., & Thomas, R. M. (2012). Validation of X-ray fluorescence spectrometry for determining osseous or dental origin of unknown material. *Journal of Forensic Sciences*, 57(1), 47-51.
10. Gilpin, M., & Christensen, A. M. (2015). Elemental Analysis of Variably Contaminated Cremains Using X-ray Fluorescence Spectrometry. *Journal of Forensic Sciences*, 60(4), 974-978. doi:10.1111/1556-4029.12757
11. Kuzel, A. R., Christensen, A. M., & Marvin, S. M. (2016). Calcium and Phosphorus Detection Using Benchtop Versus Handheld X-ray Fluorescence Spectrometers. *Journal of Forensic Sciences*, 61, S190-S192.
12. Nganvongpanit, K., Buddhachat, K., Klinhom, S., Kaewmong, P., Thitaram, C., & Mahakkanukrauh, P. (2016). Determining comparative elemental profile using handheld X-ray fluorescence in humans, elephants, dogs, and dolphins: Preliminary study for species identification. *Forensic Science International*, 263, 101-106.
13. Bush, M. A., Miller, R. G., Prutsman-Pfeiffer, J., & Bush, P. J. (2007). Identification through X-ray fluorescence analysis of dental restorative resin materials: a comprehensive study of noncremated, cremated, and processed-cremated individuals. *Journal of Forensic Sciences*, 52(1), 157-165.
14. Winburn, A. P., Rubin, K. M., LeGarde, C. B., & Finlayson, J. E. (2017). Use of qualitative and quantitative techniques in the resolution of a small-scale medicolegal case of commingled human remains. *Florida Scientist*, 24-37.
15. Moncayo, S., Manzoor, S., Ugidos, T., Navarro-Villoslada, F., & Caceres, J. (2014). Discrimination of human bodies from bones and teeth remains by laser induced breakdown spectroscopy and neural networks. *Spectrochimica Acta Part B: Atomic Spectroscopy*, 101, 21-25.
16. Christopher Kendall, Anne Marie Høier Eriksen, Ioannis Kontopoulos, Matthew J. Collins, Gordon Turner-Walker, Diagenesis of archaeological bone and tooth, *Palaeogeography, Palaeoclimatology, Palaeoecology*, Volume 491, 2018, Pages 21-37, ISSN 0031-0182, <https://doi.org/10.1016/j.palaeo.2017.11.041>.

ANNEX 1: Demographic and Processing Information for Individuals Tested

Collection Time	Donor #	Sex	Date of Birth	Date of Death	Age	Placement	Recovery	~Time @ Forest (days)	FOREST Location
PHASE 1									
May-22	2019-09	M	9/15/1958	4/29/2019	60	5/6/2019	10/25/2019	172	Enclosure 1
May-22	2019-12	M	2/13/1960	9/15/2019	59	9/19/2019	10/01/2020	378	Enclosure 1
May-22	2019-16	M	3/28/1945	10/19/2019	74	10/28/2019	11/6/2020	385	Enclosure 1
May-22	2019-20	F	3/30/1948	12/18/2019	71	12/27/2019	9/18/2020	266	Enclosure 1
May-22	2020-01	M	9/18/1947	12/28/2019	72	1/6/2020	4/16/2021	466	Enclosure 1
May-22	2020-02	F	11/17/1944	1/2/2020	75	1/13/2020	9/24/2021	620	Enclosure 1
May-22	2020-03	F	10/8/1944	1/11/2020	75	1/15/2020	9/7/2020	236	Enclosure 1
May-22	2020-06	F	7/10/1948	2/3/2020	71	2/14/2020	1/26/2021	347	Enclosure 1

This resource was prepared by the author(s) using Federal funds provided by the U.S. Department of Justice. Opinions or points of view expressed are those of the author(s) and do not necessarily reflect the official position or policies of the U.S. Department of Justice.

This resource was prepared by the author(s) using Federal funds provided by the U.S. Department of Justice. Opinions or points of view expressed are those of the author(s) and do not necessarily reflect the official position or policies of the U.S. Department of Justice.

May-22	2020-07	M	7/8/1951	3/7/2020	68	4/2/2020	11/5/2021	582	Enclosure 1
May-22	2020-08	F	10/10/1940	7/13/2020	79	8/13/2020	4/30/2021	260	Enclosure 1
May-22	2020-11	M	7/14/1966	10/6/2020	54	10/15/2020	11/5/2021	386	Enclosure 1
May-22	2021-01	F	2/27/1938	2/15/2021	82	3/8/2021	10/1/2021	207	Enclosure 1
PHASE 2									
Nov-22	2018-15	M	9/23/1945	11/27/2018	73	12/17/2018	9/13/2021	270	Enclosure 1
Nov-22	2019-01	F	2/10/1946	12/25/2018	72	1/3/2019	2/14/2022	407	Enclosure 1
Nov-22	2019-02	F	8/27/1946	1/20/2021	72	1/25/2021	9/6/2019	244	Enclosure 1
Nov-22	2019-04	M	1/29/1962	2/2/2019	57	2/11/2021	8/9/2019	179	Enclosure 1
Nov-22	2019-08	M	9/6/1988	4/29/2021	30	5/1/2019	9/6/2019	128	Enclosure 1
Nov-22	2019-14	F	5/21/1941	10/18/2019	78	10/23/2019	10/21/2021	729	Enclosure 1

This resource was prepared by the author(s) using Federal funds provided by the U.S. Department of Justice. Opinions or points of view expressed are those of the author(s) and do not necessarily reflect the official position or policies of the U.S. Department of Justice.

This resource was prepared by the author(s) using Federal funds provided by the U.S. Department of Justice. Opinions or points of view expressed are those of the author(s) and do not necessarily reflect the official position or policies of the U.S. Department of Justice.

Nov-22	2019-15	M	12/20/1965	10/21/2019	53	10/25/2019	11/1/2021	738	Enclosure 1
Nov-22	2019-19	F	1/20/1933	12/9/2019	86	12/11/2019	10/9/2020	606	Enclosure 1
Nov-22	2019-21	F	9/7/1934	12/24/2019	85	1/13/2020	9/11/2020	242	Enclosure 1
Nov-22	2020-04	M	9/30/1946	1/18/2020	73	1/22/2020	11/30/2021	678	Enclosure 1
Nov-22	2020-05	F	11/15/1930	1/16/2020	89	1/27/2020	4/9/2021	438	Enclosure 1
Nov-22	2020-09	M	6/24/1950	8/27/2020	70	9/7/2020	3/15/2022	554	Enclosure 1
Nov-22	2020-12	F	9/27/1970	10/11/2020	50	10/19/2020	7/2/2021	256	Enclosure 1
Nov-22	2020-13	M	5/17/1958	11/10/2020	62	11/19/2020	2/1/2022	439	Enclosure 1
Nov-22	2021-04	F	12/25/1966	3/4/2021	54	5/17/2021	11/9/2021	177	Enclosure 1
Nov-22	2021-05	F	7/26/1956	4/30/2021	64	5/17/2021	10/1/2021	138	Enclosure 1
Nov-22	2021-06	F	6/25/1966	5/11/2021	54	5/24/2021	11/16/2021	177	Enclosure 1

This resource was prepared by the author(s) using Federal funds provided by the U.S. Department of Justice. Opinions or points of view expressed are those of the author(s) and do not necessarily reflect the official position or policies of the U.S. Department of Justice.

This resource was prepared by the author(s) using Federal funds provided by the U.S. Department of Justice. Opinions or points of view expressed are those of the author(s) and do not necessarily reflect the official position or policies of the U.S. Department of Justice.

Nov-22	2021-03	M	3/10/1954	3/8/2021	66	3/17/2021	11/19/2021	248	Enclosure 1
PHASE									
3									
May-23	2018-08	M	11/25/1942	8/13/2018	75	8/16/2018	7/8/2020	692	Enclosure 1
May-23	2018-09	M	7/22/1958	8/17/2018	60	8/20/2018	9/13/2019	389	Enclosure 1
May-23	2018-10	M	5/13/1962	8/15/2018	56	8/22/2018	3/6/2019	196	Enclosure 1
May-23	2018-11	M	12/29/1948	9/15/2018	70	9/24/2018	9/20/2019	361	Enclosure 1
May-23	2018-14	F	3/5/1969	12/5/2018	49	2/6/2019	11/8/2019	275	Enclosure 1
May-23	2019-5	F	9/3/1949	2/5/2019	69	2/15/2019	8/9/2019	175	Enclosure 1
May-23	2019-6	F	11/12/1986	2/4/2019	32	2/15/2019	10/4/2019	231	Enclosure 1
May-23	2019-7	F	12/31/1990	3/21/2019	28	4/1/2019	8/30/2019	151	Enclosure 1
May-23	2019-10	F	6/4/1951	4/6/2019	67	5/23/2019	9/13/2019	113	Enclosure 1

This resource was prepared by the author(s) using Federal funds provided by the U.S. Department of Justice. Opinions or points of view expressed are those of the author(s) and do not necessarily reflect the official position or policies of the U.S. Department of Justice.

This resource was prepared by the author(s) using Federal funds provided by the U.S. Department of Justice. Opinions or points of view expressed are those of the author(s) and do not necessarily reflect the official position or policies of the U.S. Department of Justice.

May-23	2019-13	F	5/7/1971	9/23/2019	48	9/25/2019	7/15/2020	294	Enclosure 1
May-23	2019-17	M	11/25/1952	11/8/2019	66	11/15/2019	2/8/2022	861	Enclosure 1
May-23	2019-18	F	11/24/1955	11/20/2019	64	11/25/2019	2/8/2022	871	Enclosure 1
May-23	2021-03	M	3/10/1954	3/8/2021	66	3/17/2021	11/19/2021	247	Enclosure 1
May-23	2021-09	F	4/15/1937	5/20/2021	84	6/8/2021	2/15/2022	252	Enclosure 1
May-23	2021-11	F	5/30/1960	6/24/2021	61	6/30/2021	11/16/2021	139	Enclosure 1
May-23	2021-15	M	11/17/1954	10/13/2021	66	10/22/2021	2/1/2023	467	Enclosure 1
PHASE 4									
Nov-23	2017-18	F	5/17/1933	10/20/2017	84	10/27/2017	3/22/2019	511	Enclosure 1
Nov-23	2017-18	F	5/17/1933	10/20/2017	84	10/27/2017	3/22/2019	511	Enclosure 1
Nov-23	2018-01	M	1/17/1938	1/16/2018	79	1/23/2018	11/27/2018	308	Enclosure 1

This resource was prepared by the author(s) using Federal funds provided by the U.S. Department of Justice. Opinions or points of view expressed are those of the author(s) and do not necessarily reflect the official position or policies of the U.S. Department of Justice.

This resource was prepared by the author(s) using Federal funds provided by the U.S. Department of Justice. Opinions or points of view expressed are those of the author(s) and do not necessarily reflect the official position or policies of the U.S. Department of Justice.

Nov-23	2018-02	M	1/2/1952	1/10/2018	66	1/24/2018	8/28/2018	216	Enclosure 1
Nov-23	2018-03	M	2/10/1953	4/3/2018	65	4/9/2018	8/22/2018	135	Enclosure 1
Nov-23	2018-04	F	1/9/1941	4/23/2018	77	5/1/2018	9/18/2018	140	Enclosure 1
Nov-23	2018-05	F	11/10/1933	5/11/2018	84	5/17/2018	8/20/2018	95	Enclosure 1
Nov-23	2018-06	M	6/25/1927	5/27/2018	90	6/1/2018	8/30/2018	448	Enclosure 1
Nov-23	2018-07	F	5/31/1970	7/26/2018	48	8/9/2018	3/29/2019	232	Enclosure 1
Nov-23	2021-02	M	7/23/1940	2/22/2021	80	3/10/2021	3/1/2022	356	Enclosure 1
Nov-23	2021-10	M	9/20/1957	6/2/2021	63	6/10/2021	2/15/2022	250	Enclosure 1
Nov-23	2022-01	F	9/19/1921	1/19/2022	10	5/16/2022	9/23/2022	130	Enclosure 1
Nov-23	2022-12	M	1/30/1971	5/5/2022	51	5/10/2022	4/12/2023	337	Enclosure 1
Nov-23	2022-13	F	9/2/1966	5/10/2022	55	5/12/2022	7/27/2022	77	Enclosure 1

This resource was prepared by the author(s) using Federal funds provided by the U.S. Department of Justice. Opinions or points of view expressed are those of the author(s) and do not necessarily reflect the official position or policies of the U.S. Department of Justice.

This resource was prepared by the author(s) using Federal funds provided by the U.S. Department of Justice. Opinions or points of view expressed are those of the author(s) and do not necessarily reflect the official position or policies of the U.S. Department of Justice.

Nov-23	2022-17	M	7/18/1949	5/24/2022	72	5/27/2022	6/28/2022	398	Enclosure 1
Nov-23	2022-19	M	6/25/1963	6/14/2022	58	7/5/2022	7/19/2022	380	Enclosure 1
Nov-23	2018-13	F	11/18/1948	11/5/2021	69	11/9/2021	5/26/2022	1660	Encl 2; BURIAL

This resource was prepared by the author(s) using Federal funds provided by the U.S. Department of Justice. Opinions or points of view expressed are those of the author(s) and do not necessarily reflect the official position or policies of the U.S. Department of Justice.

This resource was prepared by the author(s) using Federal funds provided by the U.S. Department of Justice. Opinions or points of view expressed are those of the author(s) and do not necessarily reflect the official position or policies of the U.S. Department of Justice.

ANNEX 2: List of bone locations sampled for each bone

Cranium

- Frontal
- Bregma
- Lambda
- Right parietal
- Left parietal
- Right temporal
- Left temporal
- Left occipital, inferior portion
- External occipital protuberance
- Left zygomatic arch

Mandible

- Mental eminence
- Right horizontal ramus
- Right vertical ramus
- Left horizontal ramus
- Left mandibular condyle, posterior

Sternum

- Anterior manubrium
- Anterior body

This resource was prepared by the author(s) using Federal funds provided by the U.S. Department of Justice. Opinions or points of view expressed are those of the author(s) and do not necessarily reflect the official position or policies of the U.S. Department of Justice.

This resource was prepared by the author(s) using Federal funds provided by the U.S. Department of Justice. Opinions or points of view expressed are those of the author(s) and do not necessarily reflect the official position or policies of the U.S. Department of Justice.

- Anterior xiphoid process
- Posterior manubrium
- Posterior body

Clavicle

- Sternal facet
- Superior sternal third
- Inferior sternal third
- Superior midshaft
- Superior acromial third
- Conoid tubercle
- Acromial facet

Scapula

- Posterior inferior angle
- Infraspinous fossa, medial
- Infraspinous fossa, lateral
- Anterior superior angle
- Glenoid fossa
- Acromion process
- Anterior inferior angle
- Subscapular fossa, lateral
- Subscapular fossa, medial
- Coracoid process

This resource was prepared by the author(s) using Federal funds provided by the U.S. Department of Justice. Opinions or points of view expressed are those of the author(s) and do not necessarily reflect the official position or policies of the U.S. Department of Justice.

This resource was prepared by the author(s) using Federal funds provided by the U.S. Department of Justice. Opinions or points of view expressed are those of the author(s) and do not necessarily reflect the official position or policies of the U.S. Department of Justice.

Rib 1

- Scalene tubercle
- Inferior costal angle
- Articular facet
- Superior sternal end

Rib 2

- Serratus anterior tuberosity
- Superior sternal end
- Inferior sternal end
- Articular facet

Humerus, right and left

- Humeral head
- Greater tubercle
- Posterior proximal third
- Anterior midshaft
- Posterior distal end
- Anterior distal end
- Capitulum
- Deltoid tuberosity
- Medial Epicondyle

Ulna, right and left

- Olecranon process

This resource was prepared by the author(s) using Federal funds provided by the U.S. Department of Justice. Opinions or points of view expressed are those of the author(s) and do not necessarily reflect the official position or policies of the U.S. Department of Justice.

This resource was prepared by the author(s) using Federal funds provided by the U.S. Department of Justice. Opinions or points of view expressed are those of the author(s) and do not necessarily reflect the official position or policies of the U.S. Department of Justice.

- Posterior proximal end
- Posteromedial midshaft
- Radial notch
- Ulnar head
- Styloid process
- Anterior distal end
- Anterior midshaft
- Medial distal end

Radius, right and left

- Radial head
- Radial tuberosity
- Anterior midshaft
- Anterior distal third
- Posterior distal third
- Posterior midshaft
- Styloid process

Metacarpal 1

- Posterior midshaft
- Head
- Facet for trapezium

Hand Proximal Phalanx 1

- Base/facet for MC1

This resource was prepared by the author(s) using Federal funds provided by the U.S. Department of Justice. Opinions or points of view expressed are those of the author(s) and do not necessarily reflect the official position or policies of the U.S. Department of Justice.

This resource was prepared by the author(s) using Federal funds provided by the U.S. Department of Justice. Opinions or points of view expressed are those of the author(s) and do not necessarily reflect the official position or policies of the U.S. Department of Justice.

- Posterior midshaft

Hand Distal Phalanx 1

- Posterior surface
- Anterior surface

Metacarpal 3

- Posterior midshaft
- Head
- Proximal medial end/styloid

Cervical Vertebra 1

- Right inferior facet
- Left inferior facet
- Anterior arch, right
- Left transverse process

Cervical Vertebra 2

- Dens
- Right superior facet
- Left inferior facet
- Right lamina

Thoracic Vertebra 11

- Superior body
- Inferior body

This resource was prepared by the author(s) using Federal funds provided by the U.S. Department of Justice. Opinions or points of view expressed are those of the author(s) and do not necessarily reflect the official position or policies of the U.S. Department of Justice.

This resource was prepared by the author(s) using Federal funds provided by the U.S. Department of Justice. Opinions or points of view expressed are those of the author(s) and do not necessarily reflect the official position or policies of the U.S. Department of Justice.

- Spinous process tip
- Right transverse process

Lumbar Vertebra 4

- Superior body/rim
- Inferior body/rim
- Right inferior articular facet
- Anterior surface of body

Sacrum

- Anterior S1, midline
- Right auricular surface
- Facet for coccyx
- Right Ala
- Centrum

Os Coxa

- Iliac tubercle
- Posterior superior iliac spine, lateral
- Posterior inferior iliac spine, lateral
- Anterior superior iliac spine, lateral
- Ischial tuberosity
- Iliopubic ramus
- Anterior superior iliac spine, medial
- Pubic symphysis

This resource was prepared by the author(s) using Federal funds provided by the U.S. Department of Justice. Opinions or points of view expressed are those of the author(s) and do not necessarily reflect the official position or policies of the U.S. Department of Justice.

This resource was prepared by the author(s) using Federal funds provided by the U.S. Department of Justice. Opinions or points of view expressed are those of the author(s) and do not necessarily reflect the official position or policies of the U.S. Department of Justice.

- Auricular surface
- Acetabular margin

Femur, right and left

- Head
- Trochanteric line
- Greater trochanter
- Lesser trochanter
- Anterior proximal third
- Anterior midshaft
- Anterior distal third
- Spiral line area
- Medial midshaft
- Lateral midshaft
- Popliteal surface
- Medial condyle
- Lateral condyle

Tibia, right and left,

- Popliteal surface
- Fibular articular facet
- Superior articular facet on lateral condyle
- Tibial tuberosity
- Lateral midshaft

This resource was prepared by the author(s) using Federal funds provided by the U.S. Department of Justice. Opinions or points of view expressed are those of the author(s) and do not necessarily reflect the official position or policies of the U.S. Department of Justice.

This resource was prepared by the author(s) using Federal funds provided by the U.S. Department of Justice. Opinions or points of view expressed are those of the author(s) and do not necessarily reflect the official position or policies of the U.S. Department of Justice.

- Medial midshaft
- Anterior distal third
- Posterior distal third
- Talar articular surface
- Medial malleolus

Fibula, right and left

- Lateral malleolus
- Distal third, medial
- Posterior midshaft
- Lateral surface
- Fibular neck
- Tibial facet/styloid

Talus

- Trochlea
- Head
- Anterior subtalar facet

Calcaneus

- Calcaneal tuberosity
- Sustentaculum tali
- Talar facet
- Facet for cuboid

Metatarsal 1

This resource was prepared by the author(s) using Federal funds provided by the U.S. Department of Justice. Opinions or points of view expressed are those of the author(s) and do not necessarily reflect the official position or policies of the U.S. Department of Justice.

This resource was prepared by the author(s) using Federal funds provided by the U.S. Department of Justice. Opinions or points of view expressed are those of the author(s) and do not necessarily reflect the official position or policies of the U.S. Department of Justice.

- Facet for cuneiform
- Medial surface
- Superior surface
- Head

Foot Proximal Phalanx 1

- Superior surface
- Inferior surface

Foot Distal Phalanx 1

- Inferior surface
- Tuft/distal end

Metatarsal 5

- Facet for cuboid
- Superior proximal end
- Inferior distal end

